Magnetoresistance in low-temperature grown molecular-beam epitaxial GaAs

J. Betko, M. Morvic, J. Novák, A. Förster, and P. Kordoš

Citation: Journal of Applied Physics **86**, 6243 (1999);
View online: https://doi.org/10.1063/1.371679
View Table of Contents: http://aip.scitation.org/toc/jap/86/11
Published by the American Institute of Physics

Magnetoresistance in low-temperature grown molecular-beam epitaxial GaAs

J. Betko,[a] M. Morvic, and J. Novák
Institute of Electrical Engineering, Slovak Academy of Sciences, SK-84239 Bratislava, Slovakia

A. Förster and P. Kordoš
Institute of Thin Film and Ion Technology, Research Centre Jülich, D-52425 Jülich, Germany

(Received 19 May 1999; accepted for publication 18 August 1999)

Conductivity, Hall effect as well as ''physical'' and ''geometrical'' magnetoresistances were measured at 290–440 K in molecular-beam epitaxial GaAs layers grown at 200–400 °C. The experimental data were analyzed taking into account the combined band and hopping conductance regime. Positive hopping magnetoresistance parameters $(\Delta\rho/\rho_0 B^2)_h \approx 10^{-4}\,\mathrm{T}^{-2}$ and hopping Hall mobilities lower than $1\times10^{-4}\,\mathrm{m^2\,V^{-1}\,s^{-1}}$ were determined in the as-grown layers. A transverse-to-longitudinal hopping magnetoresistance ratio of about 2, consistent with hopping transport theories, was obtained. In the annealed layer grown at 200 °C (J200a) the band mobility determined from the geometrical magnetoresitance (GMR) mobility was found to be significantly higher than the band Hall mobility. It is related to a mixed band conductivity regime with the hole concentration p exceeding the electron one n. The difference between GMR and Hall mobilities decreases with increasing growth temperature as far as a typical single-carrier band conductivity regime ($n>p$) is present in the layer grown at 400 °C. In contradiction to the layers grown at higher temperatures, the J200a layer showed the opposite (positive) sign of the hopping Hall coefficient as well as the largest hopping magnetoresistance parameter ($\approx 3\times10^{-2}\,\mathrm{T}^{-2}$). © *1999 American Institute of Physics.* [S0021-8979(99)09022-2]

I. INTRODUCTION

Low-temperature (LT) grown molecular-beam epitaxial (MBE) GaAs material has attracted interest from both the physics and the application points of view.[1] Analysis of its electrical parameters using the combined band and hopping conduction model is commonly used to obtain the individual band and hopping transport parameters.[2,3] In spite of the attention paid to the study of the electrical properties of this material, there is a lack of published data concerning the galvanomagnetic parameters, especially the magnetoresistance in the hopping dominated LT GaAs. The hopping conduction magnetoresistance was studied theoretically by Mikoshiba[4] and Shklovskii[5] in simple semiconductors with the impurity state represented by the hydrogenic wave function. Experimental results were published for Ge and GaAs at low temperatures.[6,7] Recently, a theory for hopping transport in a magnetic field and its application to the calculation of the Hall mobility and the magnetoconductivity in a three-dimensional system were presented by Bleibaum *et al.*[8] Concerning LT GaAs, a giant magnetoresistance effect was observed by Wellmann *et al.* in a low-temperature grown GaAs with imbedded MnAs nanomagnets.[9]

In this work, we analyze the temperature dependent conductivity and Hall effect, as well as the transverse and longitudinal magnetoresistances in molecular-beam epitaxial GaAs layers grown at 200–400 °C, taking into account the combined band and hopping conductance regime in the samples examined. The band conduction obtained is further analyzed with respect to the mixed conductivity regime assuming both electron as well as hole conductivities.

II. EXPERIMENT DETAILS

The LT GaAs layers were grown in a Varian Mod GEN II MBE system on indium-free-mounted (100) semi-insulating GaAs wafers at substrate temperatures of 200, 250, 300, 350, and 400 °C (thermocouple reading only); the layers are denoted J200, J250, J300, J350, and J400, respectively. An As_4/Ga beam-equivalent pressure ratio of 19 and a growth rate of 1 μm/h were used to grow 2 μm thick layers. A part of each wafer was annealed using rapid thermal processing under local As overpressure at 590 °C for 10 min (the annealed layers are denoted by the additional character a). Samples of about 6×6 mm^2 were cut from the wafers, and the layers were separated from the substrate (an AlAs interlayer was grown between the substrate and the layer).[10]

Three types of sample configuration were used. For the conductivity and Hall effect measurements using the van der Pauw (vdP) method, square shaped samples were prepared with four contacts in the corners [vdP configuration, Fig. 1(a)]. Short samples (distance between the contacts of about 0.5 mm) with two wide contacts ($\cong$6 mm) were made for the ''geometrical'' magnetoresistance measurement [(GMR) configuration, Fig. 1(b)]. Finally, long bar samples of about 6×0.5 mm^2 with two contacts at the bar ends were prepared for the ''physical'' magnetoresistance measurement [(PMR) configuration, Fig. 1(c)]. The samples of all configurations

[a]Electronic mail: elekjbet@savba.sk

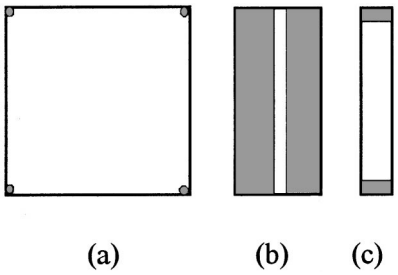

FIG. 1. Sample configurations for van der Pauw (a), geometrical magnetoresistance (b), and physical magnetoresistance (c) measurements.

were prepared consecutively from the same piece of the layer used first for the vdP measurement.

The contacts were prepared by rubbing Ga+In into the surface of the layer at room temperature, and their ohmic behavior was confirmed by current–voltage characteristics. Precise dc measurements were carried out with the samples in the dark at 290–440 K, using a high impedance system. Magnetic fields below 1 T perpendicular to the plane of the layer (perpendicular to the current) were applied to obtain the transverse GMR and PMR magnetoresistance parameters. For the longitudinal PMR magnetoresistance measurements a magnetic field parallel to the current was applied.

The combined hopping and band conductance regime is considered to be present in the LT GaAs layers investigated. Assuming that both the hopping and the band conductances are localized in the same layer, the individual conductivities were calculated for the same layer thickness. The experimental data were analyzed by using a fitting procedure with the formulas presented in the Appendix.

III. EXPERIMENTAL RESULTS

The change in the sample resistance R, upon applying a low transverse magnetic field B, can be expressed by a magnetoresistance parameter as follows:

$$S=(\Delta R/R_0B^2)_{B\to 0}, \tag{1}$$

where $\Delta R/R_0=(R_B-R_0)/R_0$ is the relative magnetoresistance (subscripts B and 0 are for values with and without applying the magnetic field, respectively). For the physical (S_{PMR}) and geometrical (S_{GMR}) magnetoresistance parameters corresponding to the PMR and GMR sample configurations, respectively, the relationships presented previously for the mixed conduction semiconductors[11–13] can be rewritten as follows:

$$S_{\mathrm{GMR}}=S_{\mathrm{PMR}}+\mu_H^2, \tag{2}$$

$$S_{\mathrm{PMR}}=S_{\mathrm{PMR},m}+S_{\mathrm{PMR},s}, \tag{3}$$

$$S_{\mathrm{PMR},m}=\sigma_b\sigma_h(R_{Hb}\sigma_b-R_{Hh}\sigma_h)^2/(\sigma_b+\sigma_h)^2, \tag{4}$$

$$S_{\mathrm{PMR},s}\cong[\sigma_b(\Delta\rho/\rho_0B^2)_b+\sigma_h(\Delta\rho/\rho_0B^2)_h]/(\sigma_b+\sigma_h), \tag{5}$$

where σ is the conductivity, R_H is the Hall coefficient (subscripts b and h are for band and hopping quantities, respectively), μ_H is the apparent Hall mobility (see Appendix), $S_{\mathrm{PMR},m}$ is the mixed conductivity term, and $S_{\mathrm{PMR},s}$ is a single-conductivity term representing the contributions of the single-band and single-hopping magnetoresistances [$\Delta\rho/\rho_0=(\rho_B-\rho_0)/\rho_0$ for $B\to 0$, ρ is the resistivity]. In general, a large difference between S_{GMR} and μ_H^2 ($S_{\mathrm{GMR}}\gg\mu_H^2$) indicates a mixed conduction regime ($S_{\mathrm{PMR},m}\gg\mu_H^2$) and/or a large contribution of the single-conduction magnetoresistances ($S_{\mathrm{PMR},s}\gg\mu_H^2$).

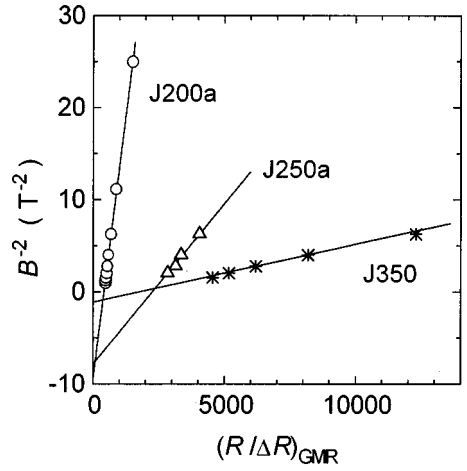

FIG. 2. Square of the inverse magnetic field vs inverse GMR magnetoresistance at room temperature for one as-grown (J350) and two annealed (J200a and J250a) samples. The solid lines are linear fits.

For the low magnetic field the quadratic field dependence of the band conductivity is assumed:

$$(\sigma_b)_B=\sigma_{b0}(1-q_b\mu_{Hb}^2B^2), \tag{6}$$

which yields a band magnetoresistance per B^2 as follows:

$$(\Delta\rho/\rho_0B^2)_b\cong q_b\mu_{Hb}^2, \tag{7}$$

where q_b is a magnetoresistance coefficient which is identical to the physical magnetoresistance coefficient ξ in the case of the single-carrier band conduction regime (theoretical values of ξ between 0.0865 and 0.577 were presented by Look for various scattering mechanisms).[11] $q_b\gg\xi$ indicates that a mixed band conduction regime is present.

To analyze the experimental data successfully, it is necessary to determine the magnetoresistance parameters as well as the Hall effect at a sufficiently low magnetic field or to extrapolate them to $B\to 0$ [see Eq. (1)]. It is important to meet this requirement especially in the case of the combined conduction, in which case these quantities can depend on the magnetic field very strongly. Fortunately, the magnetoresistance experimental data fulfilled well a linear dependence $1/B^2$ vs $R_0/\Delta R$.[11] In Figs. 2 and 3 the above dependence measured at room temperature is plotted for some samples of GMR and PMR configurations, respectively. The slopes of the $1/B^2$ vs $R_0/\Delta R$ plots for the GMR and PMR sample configurations are equivalent to the magnetoresistance parameters S_{GMR} and S_{PMR}, respectively. It should be noted that all the magnetoresistances measured were positive, i.e., the resistance of each sample under the magnetic field was greater than that without the magnetic field. The transverse and the longitudinal magnetoresistances in the as-grown J350 sample, as an example, are shown in Fig. 3. It is seen

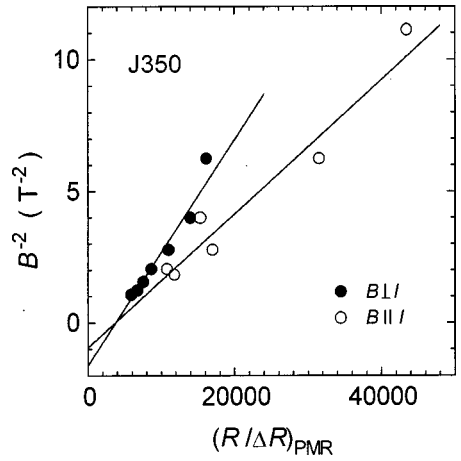

FIG. 3. Square of the inverse magnetic field vs inverse PMR transverse ($B\perp I$) and longitudinal ($B\|I$) magnetoresistances at room temperature for the as-grown J350 sample. The solid lines are linear fits.

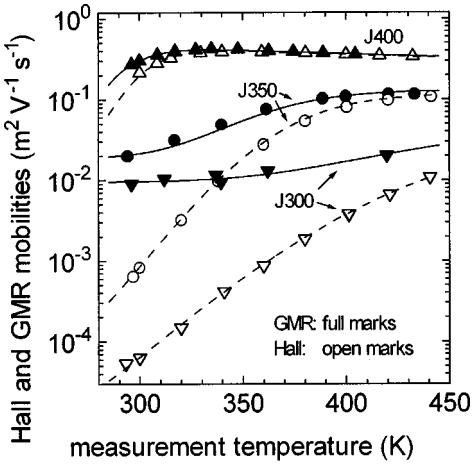

FIG. 5. Apparent Hall (open marks) and GMR (full marks) mobilities vs measurement temperature for as-grown samples grown at 300 (down triangles), 350 (circles), and 400 °C (up triangles). The dashed and solid lines are theoretical fits.

that the transverse magnetoresistance is by a factor close to 2 larger than the longitudinal one. This sample, despite the fact that its growth temperature was higher (350 °C), exhibited a hopping dominated conductance regime at room temperature, as follows from Fig. 6 below, which had also been shown in our previous work.[14] If the band conductance is dominant, the above factor will be evidently higher, e.g., a transverse-to-longitudinal magnetoresistance ratio of about 10 was found in the J400 sample.

The parameters S_{GMR}, S_{PMR}, and μ_H^2 obtained from the measurements fulfilled excellently Eq. (2), which is demonstrated for sample J350 in Fig. 4. At lower temperatures μ_H^2 is extremely small, and the PMR and GMR magnetoresistance parameters are close to each other. At the higher temperatures μ_H^2 approaches S_{GMR}, and S_{PMR} decreases.

In Fig. 5, temperature dependences of the GMR mobility defined as the root square of S_{GMR} are plotted for as-grown samples J300, J350, and J400. For comparison, the apparent Hall mobilities are also shown in Fig. 5. The corresponding zero magnetic field conductivities versus inverse measurement temperature are plotted in Fig. 6. As seen in Fig. 6, the conductivities obtained with the GMR sample configuration (two-point measurement) are in good agreement with those obtained with the vdP one. Hence, it can be deduced that the contact resistances of GMR samples are negligible. At room temperature the GMR mobility largely exceeds the apparent Hall mobility (see Fig. 5). It is associated with the combined hopping and band conductivity regime as well as with the significant single-hopping magnetoresistance. At higher measurement temperatures the band conductance becomes more dominant (see Fig. 6), and the GMR and Hall mobilities approach each other (see Fig. 5) indicating a single-carrier (*n*-type) band conductance.

In Fig. 7, the GMR and Hall mobilities versus measurement temperature are plotted for annealed samples J200a, J300a, and J400a. The data for samples J250a and J350a are not shown to preserve the clarity of the figure. The corresponding conductivities versus inverse measurement temperature are plotted in Fig. 8. It is evident (Fig. 7) that even

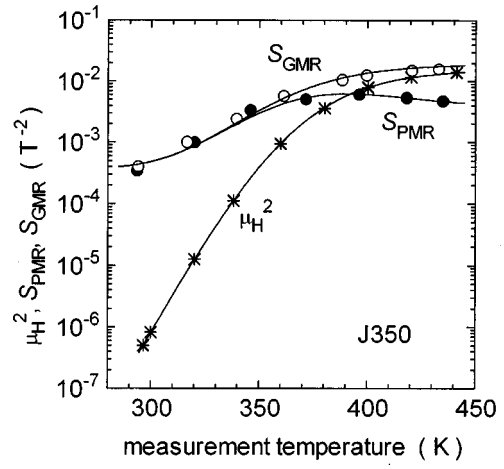

FIG. 4. Square of the apparent Hall mobility (μ_H^2) and the physical (S_{PMR}) and geometrical (S_{GMR}) magnetoresistance parameters vs measurement temperature for sample J350. The solid lines are theoretical fits.

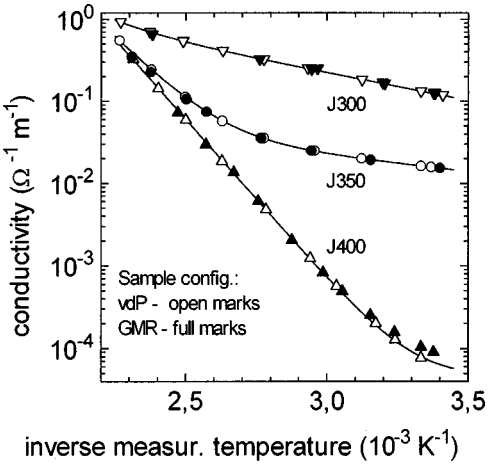

FIG. 6. Conductivity vs inverse measurement temperature for the as-grown samples in Fig. 5 obtained with the vdP (open marks) and GMR (full marks) sample configurations at $B=0$. The solid lines are theoretical fits of the vdP conductivity.

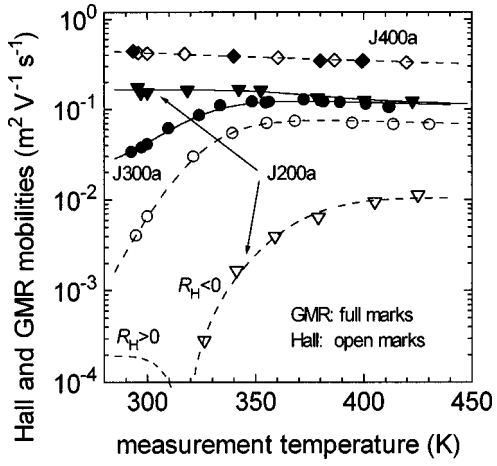

FIG. 7. Apparent Hall (open marks) and GMR (full marks) mobilities vs measurement temperature for annealed samples grown at 200 (down triangles), 300 (circles), and 400 °C (diamonds). The dashed and solid lines are theoretical fits.

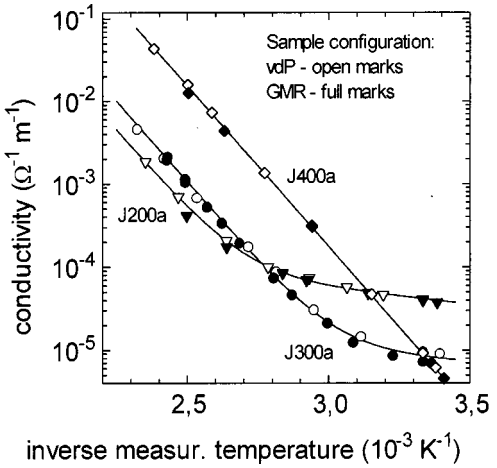

FIG. 8. Conductivity vs inverse measurement temperature for the annealed samples in Fig. 7 obtained with the vdP (open marks) and GMR (full marks) sample configurations at $B=0$. The solid lines are theoretical fits of the vdP conductivity.

at higher measurement temperatures (band dominated conductance regime) a large difference occurs between the Hall and the GMR mobilities, especially in the annealed layer grown at 200 °C (sample J200a). This sample also exhibited an enormous difference between the Hall and the GMR mobilities at lower measurement temperatures (hopping dominated conductance regime), as well as a positive sign of the hopping Hall coefficient ($R_H>0$), obtained from the fitting [see the sign of the hopping parameter $(R_{Hh}\sigma_h)_{300}$ in Table I]. For the J200a Hall data, the fit suggests that a *p*-type region should occur at lower measurement temperatures (see Fig. 7). Unfortunately, no *p*-type data could be successfully measured since in this range the voltage noise measured was relatively high compared with small Hall effect signal expected.

The dashed and full lines in Figs. 4–8 are the theoretical fits using both the combined band and hopping conductance model in the Appendix and the physical and geometrical magnetoresistance phenomena described above. The fitting procedure was applied simultaneously to the temperature dependences of all the parameters measured (conductivity, Hall mobility, and magnetoresistance). An excellent agreement between the experimental data and fitting curves is obtained, which corroborates the reliability of the analysis used. A list of the fitted parameters is presented in Table I.

IV. DISCUSSION

In the as-grown LT GaAs samples (J300, J350, and J400) and in the annealed samples grown at higher temperatures (J350a and J400a) the Hall and the GMR band mobilities are close to each other and the band magnetoresistance coefficient q_b (0.05–0.7) corresponds to the physical magnetoresistance coefficient ξ in *n*-type GaAs.[11] On the other hand, the annealed LT GaAs samples grown at temperatures below 350°C show remarkable differences between the Hall and the GMR band mobilities. For samples J200a, J250a, and J300a, band magnetoresistance coefficients $q_b=112$, 6.2, and 1.6 were obtained from the fitting procedure, respectively. This result can be explained by assuming a mixed conductivity regime with a significant role of both electrons and holes in the band transport. We analyzed the experimental data of the annealed samples grown at lower temperatures using a treatment employed previously for semi-insulating bulk GaAs,[11,15] taking into account the intrinsic carrier concentration by Blakemore[16] ($n_i=6.57\times10^{15}\,\mathrm{m}^{-3}$ at 400 K) and assuming electron and hole Hall scattering factors $r_n=1$ and $r_p=1.5$, respectively. For sample J200a, which had the largest q_b, the analysis yields the following values of the standard band parameters at 400 K (this measurement temperature was chosen because at 400 K the measured param-

TABLE I. Band and hopping parameters resulted from the fitting of equation sets (A1)–(A6) and (2)–(7) to the experimental data.

	Band parameters					Hopping parameters			
Sample	$(eR_{Hb})^{-1}_{300}$ (m^{-3})	E_{D0} (eV)	$(R_{Hb}\sigma_b)_{300}$ ($m^2 V^{-1} s^{-1}$)	m	q_b	$(eR_{Hh})^{-1}$ (m^{-3})	$(R_{Hh}\sigma_h)_{300}$ ($m^2 V^{-1} s^{-1}$)	ϵ_3 (eV)	$(\Delta\rho/\rho B^2)_h$ (T^{-2})
J300	-2.0×10^{16}	0.56	−0.043	0	0.30	-4×10^{22}	-2×10^{-5}	0.134	9×10^{-5}
J350	-5.4×10^{15}	0.64	−0.120	0	0.2	-1×10^{21}	-9×10^{-5}	0.077	4×10^{-4}
J400	-5.1×10^{14}	0.75	−0.450	0.8	<0.05				
J200a	-1.1×10^{14}	0.75	−0.013	0.5	112	$+1\times10^{18}$	$+2\times10^{-4}$	0.076	3×10^{-2}
J250a	-4.9×10^{13}	0.75	−0.048	0.5	6.2	-4×10^{19}	-1×10^{-5}	0.06	2×10^{-3}
J300a	-3.8×10^{13}	0.75	−0.091	0.7	1.6	-5×10^{18}	-1×10^{-5}	0.05	5×10^{-4}
J350a	-5.0×10^{13}	0.75	−0.160	0.6	0.7	-6×10^{17}	-1×10^{-5}	0.05	6×10^{-3}
J400a	-1.3×10^{14}	0.75	−0.423	0.7	0.2				

eters are close to the band ones): the electron to hole Hall mobility ratio $b_H \cong 12$, the electron (n) to hole (p) Hall concentration ratio $c_H \cong 0.01$ ($n \cong 7\times10^{14}\,\mathrm{m}^{-3}$ and $p \cong 7\times10^{16}\,\mathrm{m}^{-3}$), the electron Hall mobility $\mu_{Hn} \cong 0.32\ \mathrm{m}^2\,\mathrm{V}^{-1}\,\mathrm{s}^{-1}$, the physical magnetoresistance parameter $\xi \cong 0.6$, and the band-gap narrowing[17] $\Delta E_g \cong 0.03\,\mathrm{eV}$. As $c_H \ll 1$, it indicates that $N_{AA} > (N_{DD}+N_D) - N_A > 0$, where N_{AA} (N_A) and N_{DD} (N_D) are the concentrations of the deep (shallow) acceptors and donors, respectively. Ga vacancies V_{Ga} and As antisites $\mathrm{As_{Ga}}$ are usually considered to be deep acceptor- and donor-like point defects in LT GaAs, respectively.[2,18,19] Hence, it can be deduced that as the growth temperature increases from 200 to 400 °C, the annealed LT GaAs layers are gradually changed from V_{Ga} acceptor dominated to $\mathrm{As_{Ga}}$ donor dominated. Moreover, in the J200a sample the hopping Hall coefficient exhibits the opposite sign (positive) and the hopping magnetoresistance parameter is considerably higher than those in the other samples (see the hopping parameters in Table I). This also confirms the different conductance conditions in the annealed J200a sample with regard to the other ones.

The above explanation of large values of q_b suggests that: (i) the sample should be p type and (ii) all of the $\mathrm{As_{Ga}}$ defects should be ionized. The first assumption can be considered to be fulfilled, as the mixed conductivity analysis really gives $p > n$ in sample J200a. The second one seems to contradict the results by Liu *et al.*,[20] which indicate that the concentration of neutral $\mathrm{As_{Ga}}$ ($\mathrm{As^0_{Ga}}$) always dominates over the concentration of ionized $\mathrm{As_{Ga}}$ ($\mathrm{As^+_{Ga}}$) defects for 200 °C material, no matter what the annealing temperature. For a serious analysis of this discrepancy, more detailed information should be needed concerning the determination of $\mathrm{As^0_{Ga}}$, $\mathrm{As^+_{Ga}}$, and V_{Ga} concentrations in annealed LT GaAs.

On the other hand, if a single band conduction (n type) is assumed, inhomogeneity can come into question to explain the large values of q_b. However, such a large value, as measured in sample J200a ($q_b = 112$), is unlikely to be obtained if a contribution of p-type conductance is excluded. It is instructive to consider InSb–NiSb material for magnetoresistance devices,[21] which contains intentionally introduced inhomogeneities (1.8 wt. % of conductive NiSb needles) oriented in the direction of the Hall electric field. Even in this type of material the magnetoresistance coefficient q_b can be estimated to be only about 4. Moreover, if our samples J200a, J250a, and J300a were n type, their band conductivities would be higher than the near intrinsic values measured.

The mixed-conductivity model seems to be more acceptable than the inhomogeneity-based one as it explains better the large values of q_b. This is also supported by the fact that the electrical properties of samples 200a, J250a, and J300a are comparable with those of Cr-doped bulk semi-insulating GaAs, which exhibit a mixed-conductivity regime.[22] However, a special type of combined conductivity, with potential fluctuations due to inhomogeneous distribution of deep defects[23] by alternating $\mathrm{As_{Ga}}$- and V_{Ga}-dominated regions, can also come into consideration.

The hopping magnetoresistance parameter $(\Delta\rho/\rho_0 B^2)_h$ obtained from the experimental data analysis (Table I) is markedly higher than the square of the corresponding hopping Hall mobility. The magnetoresistance in the hopping conductance dominated semiconductors is explained, in general, by an influence of the magnetic field on the wave functions of the impurities.[4] Thus it can differ qualitatively from the one related to the band-like conduction, where the relative magnetoresistance is limited by $\mu^2_{Hn}B^2$. An analysis of the hopping magnetoresistance in the low transverse magnetic field was presented by Mikoshiba[4] (see also Ref. 6) and Shklovskii[24] for a simplified model represented by hydrogenic wave functions. According to their formulas, the hopping magnetoresistance is nearly inversely proportional to the donor concentration and to the electron effective mass, and it does not depend on the hopping Hall mobility. However, for a detailed analysis of the hopping magnetoresistance in LT GaAs, the hopping model should be modified taking into account the hops between deep centers with tightly bound wave functions.

Concerning the transverse-to-longitudinal magnetoresistance ratio, the result obtained (a value of about 2) is consistent with the hopping transport theories.[4,8] Mikoshiba pointed out that a longitudinal magnetoresistance appears even in an isotropic medium of hopping conduction, contrary to the zero magnetoresistance expected for band conduction.[4] He obtained a factor of 2 between the transverse and the longitudinal hopping magnetoresistances for cubic crystals. Also, according to the theory by Bleibaum *et al.* electrons which jump in the direction of the magnetic field feel the field less than in the transverse case.[8]

V. CONCLUSION

Temperature dependent magnetoresistance measurements have provided new information about the transport properties of LT GaAs layers. The magnetoresistance effects in LT GaAs layers can be described considering the concept of combined hopping and band conduction, using the formalism applied previously for bulk semi-insulating GaAs. A significant difference is found between the Hall and the GMR band mobilities, especially in the annealed sample grown at 200 °C, which could be explained by the presence of a mixed band conductivity regime. Moreover, from the analysis it follows that the sign of the hopping Hall coefficient in the annealed samples changes from positive in the sample grown at 200 °C to negative in the samples grown at higher temperatures. The hopping magnetoresistance (larger by several orders of magnitude than $\mu^2_{Hh}B^2$) as well as the transverse-to-longitudinal magnetoresistance ratio of about 2 (obtained from the experiment) are consistent with hopping conduction theories. For a detailed analysis of the hopping magnetoresistance in LT GaAs, the simple hopping model should be modified in order to take into account the presence of the deep-level defects.

ACKNOWLEDGMENTS

The authors thank Dr. M. Moško and Dr. J. Darmo for helpful discussions. This work was partially supported by Grant No. 2/4059/98 from the Slovak Grant Agency VEGA.

APPENDIX

The following well-known formulas for the total conductivity σ and the apparent Hall coefficient R_H (R_H is considered to be negative for electrons) and the definition of the apparent Hall mobility μ_H were used in the analysis (subscripts b and h are for band and hopping quantities, respectively):

$$\sigma=\sigma_b+\sigma_h, \quad R_H\sigma^2=R_{Hb}\sigma_b^2+R_{Hh}\sigma_h^2, \tag{A1}$$

$$\mu_H=|R_H\sigma|. \tag{A2}$$

Further, the equation set below was used in the fitting procedure:

$$1/eR_{Hb}=(1/eR_{Hb})_{300}(T/T_{300})^{3/2}\exp[-E_{D0}(1/kT - 1/kT_{300})], \tag{A3}$$

$$1/eR_{Hh}=\text{constant}, \tag{A4}$$

$$R_{Hb}\sigma_b=(R_{Hb}\sigma_b)_{300}(T_{300}/T)^m, \tag{A5}$$

$$R_{Hh}\sigma_h=(R_{Hh}\sigma_h)_{300}\exp[-\epsilon_3(1/kT-1/kT_{300})], \tag{A6}$$

where e is the elementary charge, T is the measurement temperature, k is Boltzmann's constant, E_{D0} is the thermal activation energy (at $T\rightarrow 0$) of the band carrier concentration[25] due to the presence of deep donor- and/or acceptor-like defects, and ϵ_3 is the activation energy of the hopping Hall mobility,[24] the subscript 300 is for room temperature values ($T=300$ K).

[1] See e.g., review in M. Missous, Mater. Sci. Eng., B **44**, 304 (1997).
[2] D. C. Look, J. Appl. Phys. **74**, 306 (1993).
[3] J. Betko, M. Morvic, J. Novák, A. Förster, and P. Kordoš, Appl. Phys. Lett. **69**, 2563 (1996).
[4] N. Mikoshiba, J. Phys. Chem. Solids **24**, 341 (1963).
[5] B. I. Shklovskii and A. L. Efros, *Electronic Properties of the Doped Semiconductors* (Nauka, Moskva, 1979), p. 219 (in Russian).
[6] W. W. Lee and R. J Sladek, Phys. Rev. **158**, 794 (1967).
[7] L. Halbo and R. J. Sladek, Phys. Rev. **173**, 794 (1968).
[8] O. Bleibaum, H. Böttger, and V. V. Bryksin, Phys. Status Solidi B **205**, 157 (1998).
[9] P. J. Wellmann, J. M. Garcia, J.-L. Feng, and P. M. Petroff, Appl. Phys. Lett. **73**, 3291 (1998).
[10] J. Novák, M. Morvic, J. Betko, A. Förster, and P. Kordoš, Mater. Sci. Eng., B **40**, 58 (1996).
[11] D. C. Look, *Electrical characterization of GaAs Materials and Devices* (Wiley, Chichester, 1989).
[12] J. Betko and K. Merínský, Phys. Status Solidi A **77**, 331 (1983).
[13] D. I. Rode, Phys. Status Solidi B **55**, 687 (1973).
[14] P. Kordoš, J. Betko, M. Morvic, J Novák, and A. Förster, in *Semiconducting and Insulating Materials*, Toulouse, 1996, edited by Ch. Fontaine (LAAS-CNRS, Toulouse, 1996), p. 37.
[15] J. Betko and K. Merínský, Phys. Status Solidi A **87**, 683 (1985).
[16] J. S. Blakemore, J. Appl. Phys. **53**, R123 (1982).
[17] L. Hrivnák, J. Appl. Phys. **62**, 3228 (1987).
[18] M. Luysberg, H. Sohn, A. Prasad, P. Specht, Z. Liliental-Weber, and E. R. Weber, J. Appl. Phys. **83**, 561 (1998).
[19] J. Darmo and F. Dubecký, in *Semi-Insulating III-V Materials*, Warsaw, 1994, edited by M. Godlewski (World Scientific, Singapore, 1994), p. 355.
[20] X. Liu, A. Prasad, W. M. Chen, A. Kurpiewski, A. Stoschek, Z. Liliental-Weber, and E. R. Weber, Appl. Phys. Lett. **65**, 3002 (1994).
[21] H. Weiss and M. Wilhelm, Z. Phys. **176**, 399 (1963) (in German).
[22] L. Hrivnák, J. Betko, and K. Merínský, in *Semi-Insulating III-V Materials* (Evian 1982), edited by S. Makram-Ebeid and B. Tuck (Shiva, Nantwich, 1982), p. 139.
[23] B. Pistoulet, P. Girard, and G. Hamamdjian, J. Appl. Phys. **56**, 2268 (1984).
[24] B. I. Shklovskii, Fiz. Tekh. Poluprovodn. (St.-Peterburg) **6**, 1197 (1972), in Russian.
[25] D. C. Look, D. C. Walters, M. O. Manasreh, J. R. Sizelove, and C. E. Stutz, Phys. Rev. B **42**, 3578 (1990).